Short communication

Percolated interface conductivity of sheet-like electrolyte prepared from poly(2-acrylamido-2-methyl-1-propanesulfonic acid)-deposited core–shell particles and effect of core particle size

Hisatoshi Sakamoto[a], Yusuke Daiko[b], Kiyofumi Katagiri[c], Hiroyuki Muto[a], Mototsugu Sakai[a], Atsunori Matsuda[a,*]

[a] Department of Materials Science, Toyohashi University of Technology, 1-1 Hibarigaoka, Tempaku, Toyohashi, Aichi 441-8580, Japan
[b] Department of Materials Science and Chemistry, University of Hyogo, Shosha, Himeji, Hyogo 670-2101, Japan
[c] Department of Applied Chemistry, Graduate School of Engineering, Nagoya University, Nagoya, Aichi 464-8603, Japan

ABSTRACT

Proton conducting poly(2-acrylamido-2-methyl-1-propanesulfonic acid) (PAMPS) ultrathin layer was deposited on sol–gel-derived phenylsilsesquioxane ($PhSiO_{3/2}$) particles via layer-by-layer (LbL) assembly technique. Spherical and size-controlled particles in the range of 0.3–4.0 µm were successfully prepared by varying the condensation reaction. One PAMPS layer with 1.5 nm thickness was deposited on the particle, the volume fractions of Primer/PAMPS-multilayer varied from 0.7 to 11 vol.%. Sheet-like composite electrolytes in which PAMPS layer percolated throughout the sample can be obtained by hot-pressing the PAMPS-deposited $PhSiO_{3/2}$ particles. The sample prepared using unmodified $PhSiO_{3/2}$ exhibited a very low proton conductivity of 10^{-9} S cm^{-1} at 80 °C, whereas the conductivity of the composite electrolytes increased significantly with a very small amount of PAMPS-multilayer ($\sim$1 vol.%). The composite with 11 vol.% PAMPS exhibited 2×10^{-3} S cm^{-1} at 80 °C and 95% of relative humidity.

© 2010 Elsevier B.V. All rights reserved.

1. Introduction

Fast-proton conducting polymer electrolytes have attracted considerable attention owing to their potential applications such as hydrogen sensors [1], capacitors [2] and fuel cells [3]. Fuel cells are considered as next generation power sources because of their high energy conversion efficiency with low environmental pollutions. Perfluorosulfonate ionomers (e.g. Nafion®) have been used as fuel cell electrolytes due to their high proton conductivity at around room temperature. However, high fabrication cost and insufficient thermal stability limit their industrial applications. This promotes great interests in developing an alternative electrolyte with high fuel cell performance and low cost.

In order to improve proton conductivity and chemical/thermal stabilities, various types of composite electrolytes have been demonstrated [4–6]. It was reported that the dispersion of inorganic particles in polymer electrolytes improved not only thermal stability but also ionic conductivity [7–10]. Croce et al. reported that the number of mobile lithium ions increased significantly by dispersing Al_2O_3 nanoparticles in polyethylene oxide matrix. On the

other hand, it has been demonstrated that nanometer-scale multilayers of solid electrolytes can realize artificial heterointerfaces, where large enhancements of ionic conductivities including those of Li$^+$ [11], F$^-$ [12], O^{2-} [13] Ag$^+$ [14] and H$^+$ [15] have also been reported.

We have prepared ultrathin, proton conducting multilayers-deposited inorganic–organic composite electrolytes for fuel cells [16–19]. Proton conductors a few nanometers in thickness were deposited on sol–gel-derived phenylsilsesquioxane ($PhSiO_{3/2}$) particles via layer-by-layer (LbL) assembly technique. The $PhSiO_{3/2}$ particle has a plastic deformation property [17,19], and sheet-like composite electrolytes can be obtained from the resultant core–shell particles by hot-pressing. The sheet-like electrolyte consisting of core–shell particles deposited with highly proton-conductive poly(2-acrylamido-2-methyl-1-propanesulfonic acid) (PAMPS) exhibited the proton conductivity of 5.4×10^{-4} S cm^{-1} at 80 °C and 80% of relative humidity (RH). It was found that the proton conductivity of the sheet-like electrolytes increased with increasing the number of deposited PAMPS layers (n) up to n = 3, whereas the conductivities tended to level off from n = 3 to 5 [19]. Extension and percolation of the proton conducting path (PAMPS nanolayer) in the sheet-like composite electrolytes is crucial to achieve high proton conductivities.

In this study, the volume fractions of PAMPS-multilayer in the composite electrolytes were controlled by changing the size of the

* Corresponding author. Tel.: +81 532 44 6799; fax: +81 532 48 5833.
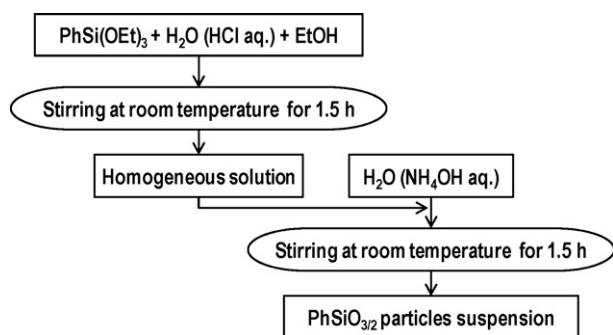*E-mail address:* matsuda@tutms.tut.ac.jp (A. Matsuda).

Fig. 1. Preparation procedure of PhSiO$_{3/2}$ particles.

core particle. Proton conductivities of composite electrolytes prepared using the PAMPS-deposited PhSiO$_{3/2}$ particles are discussed in relation to the volume fraction and percolation of proton conducting multilayers.

2. Experimental

2.1. Preparation of PhSiO$_{3/2}$ particles and size control

Phenyltriethoxysilane (PhSi(OEt)$_3$) (Shin-Etsu Chemical Co., Ltd.,) was used as a starting material. Hydrochloric acid (HCl) of 0.1 mass% and various concentrations of ammonia water (NH$_4$OH, 1–28 mass%) were used as catalysts for hydrolysis and condensation reactions, respectively. Preparation procedures of core particles are shown in Fig. 1. The molar ratio of PhSi(OEt)$_3$:H$_2$O(in HCl solution):ethanol(EtOH) was fixed to be 1:40:25. The molar ratio of NH$_4$OH used was summarized in Table 1.

2.2. Preparation of PAMPS-deposited core–shell particles

Poly(diallyldimethylammonium chloride) (PDDA, weight-average molecular mass $M = 100,000–200,000$ g mol^{-1}, Aldrich) and poly(sodium 4-styrenesulfonate) (PSS, weight-average molecular mass $M = 70,000$ g mol^{-1}, Aldrich) were used as a polycation and a polyanion for LbL, respectively. Poly(2-acrylamido-2-methyl-1-propanesulfonic acid) (PAMPS, weight-average molecular mass $M = 2,000,000$ g mol^{-1}, Aldrich) was used as a proton conductor. Since the obtained PhSiO$_{3/2}$ particles are negatively charged, at first PDDA(+) and then PSS(−) layers were deposited on the particles alternately as primer layers to increase the surface charge density. The PDDA(+)/PSS(−)/PDDA(+)/PAMPS(−) multilayer was formed. Detailed deposition procedures are shown in our previous study [19].

2.3. Characterization

The morphology and particle size were examined by a field emission scanning electron microscopy (FE-SEM, S-4800, Hitati High-Technologies). Solid-state ^{29}Si magic-angle spinning (MAS) NMR measurements were carried out using a Varian Unity 400 plus instrument. The NMR spectra were measured at 79.45 MHz, 6.7 μs of 90° pulse length, 15 s of decay time between pulses, and a spinning rate 3000–4000 Hz. A quartz crystal microbalance (QCM, HP53131A, USI) was used to measure the amount of each layer. A gold-evaporated QCM electrode (AT-cut) with the resonance frequency of 9 MHz was used. The QCM electrode was cleaned using piranha solution (98% H$_2$SO$_4$: 30% H$_2$O$_2$ = 3:1, v/v), rinsed with pure water, and then dried with nitrogen gas. After the cleaning, the electrode was rinsed with pure water and then dried with nitrogen gas.

Sheet-like samples were prepared from the PAMSP-deposited PhSiO$_{3/2}$ particles by pressing under 70 MPa at room temperature and then hot-pressing under 2 MPa at 120 °C for 1 min. The proton conductivity of the samples was determined from Cole–Cole plots obtained by an AC method using an impedance analyzer (SI 1260, Solartron) at frequencies ranging from 1 to 10 MHz. Gold electrodes (0.07 cm^2) were evaporated on both sides of the pelletized samples (13 mm in diameter and 0.4 mm in thickness).

3. Results and discussion

3.1. Size control of PhSiO$_{3/2}$ particle

SEM images of PhSiO$_{3/2}$ particles prepared by changing the concentration/amount of NH$_4$OH water are shown in Fig. 2, and the average particles diameters are summarized in Table 1. The coefficients of variation (CV) of the resultant particles were estimated to be 7~15%. As shown in Table 1, the size of PhSiO$_{3/2}$ particles increased with increasing the concentration of NH$_3$ of NH$_4$OH solution.

The condensation reaction of hydrolyzed PhSi(OEt)$_3$ in the sol changes by pH value, and NH$_4$OH catalyst accelerates the condensation reaction. Fig. 3 shows the NMR spectra of the resultant particles with 0.3, 1.2 and 1.8 μm sizes. The bonding of the PhSiO$_{3/2}$ is described in terms of T^n groups, where n represents the number of bridging oxygen around a silicon atom [20]. It is clear that the T^2 unit decreased with increasing the concentration of NH$_3$.

All the ^{29}Si NMR spectra shown in Fig. 3 were deconvoluted, and molar ratio (α) of the T^3 unit was calculated from the peak areas of T^2 and T^3.

$$\alpha = \frac{T^3\,(\text{peak area})}{T^2\,(\text{peak area}) + T^3\,(\text{peak area})}$$

Fig. 4 shows the relationship between the PhSiO$_{3/2}$ particle size and calculated α. A linear relation was observed between the α and particle size. This suggests that the PhSiO$_{3/2}$ network developed and the particle size became larger by increasing the NH$_3$ concentration. Spherical and size-controlled particles in the range of 0.3–4.0 μm can be successfully obtained by varying the condensation reaction.

Table 1
The NH$_4$OH solution conditions of sol–gel synthesis and the average particle diameter of PhSiO$_{3/2}$.

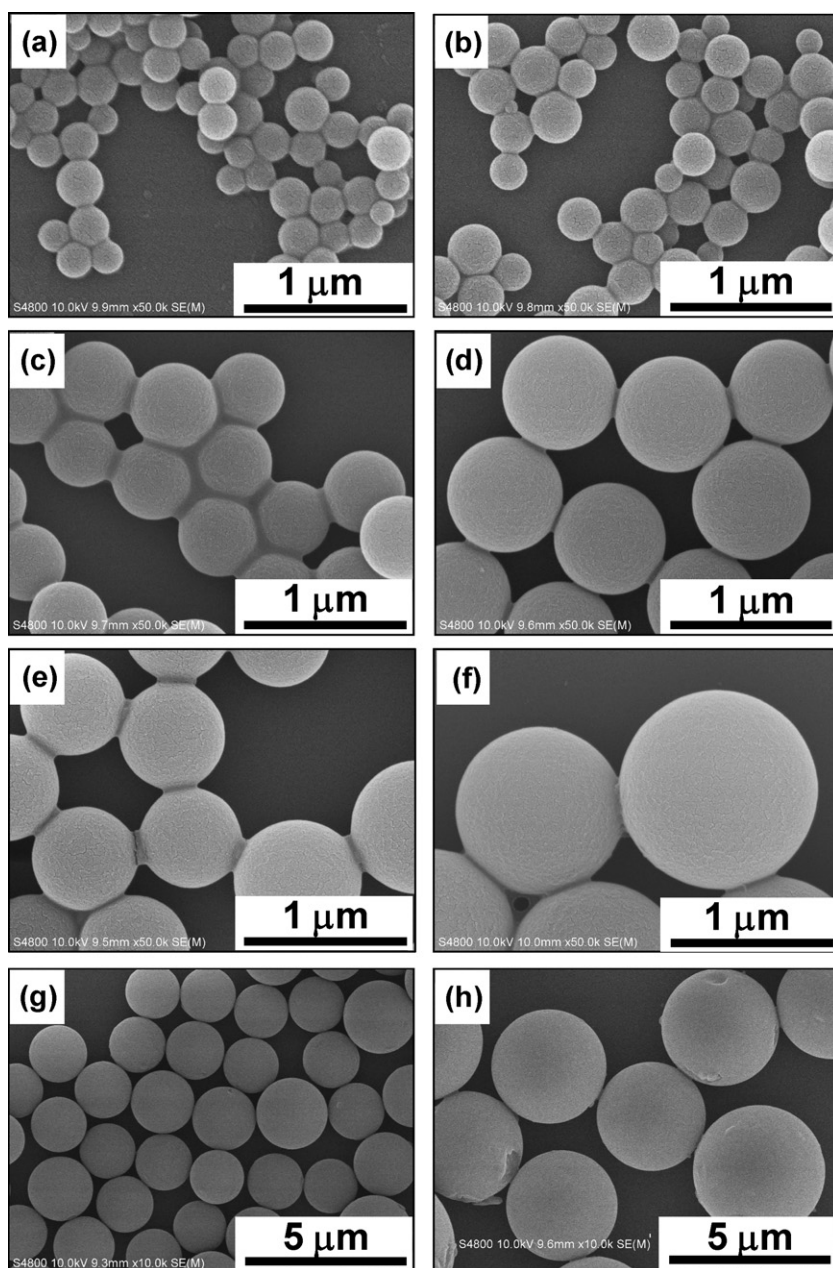|	NH$_4$OH aq.		Average particle diameter (μm)	Standard deviation (μm)	Coefficient of variation (%)
	H$_2$O molar ratio	NH$_3$ concentration (wt.%)			
(a)	500	1	0.25	0.031	13
(b)	300	1	0.3	0.037	13
(c)	200	1	0.5	0.046	10
(d)	120	4	0.7	0.070	10
(e)	100	4	0.8	0.126	15
(f)	70	10	1.2	0.149	12
(g)	50	15	1.8	0.132	7
(h)	30	28	4.0	0.328	8

Fig. 2. SEM images of size-controlled PhSiO$_{3/2}$ particles. The average particle diameters are (a) 0.25 μm, (b) 0.3 μm, (c) 0.5 μm, (d) 0.7 μm, (e) 0.8 μm, (f) 1.2 μm, (g) 1.8 μm and (h) 4.0 μm.

3.2. Proton conductivity of composites

Multilayers of PDDA/PSS/PDDA/PAMPS were deposited on the resultant PhSiO$_{3/2}$ particles via LbL technique. The amount (μg cm^{-2}) of deposited multilayer was estimated using QCM. The total thickness of the (PDDA/PSS/PDDA) multilayer was estimated to be 3.5 nm from the weight increases and densities of PDDA (1.3 g cm^{-3}) and PSS (1.3 g cm^{-3}). Similarly, the thickness of the PAMPS layer was estimated to be 1.5 nm. The density of PAMPS used in the estimation was 1.74 g cm^{-3} [21].

Changes in the proton conductivity of the sheet-like composite electrolytes with relative humidity at 80 °C are shown in Fig. 5. The proton conductivity increased with increasing the relative humidity and reached an approximately constant value at the relative humidity above 80%. PAMPS itself dissolves easily in water or humid atmosphere, whereas no deformations such as swelling or deliquescence were observed for the composites electrolytes even after the conductivity tests (80 °C and 95% RH). This is ascribed to the PAMPS layer being stabilized and fixed on the particles due to the strong electrostatic interaction between positively charged PDDA and PAMPS.

The proton conductivity measured under 80% RH is plotted in Fig. 6 as a function of reciprocal temperature. The apparent activation energies (ΔE) for proton hopping calculated from the slope in Fig. 6 are approximately 25 kJ mol^{-1} for the composites. These ΔE values suggest that protons dissociated from sulfo-groups of PAMPS are hopping through adsorbed water molecules. It is apparent from Fig. 5 and Fig. 6 that the composites consisting with smaller-sized particles showed higher proton conductivity.
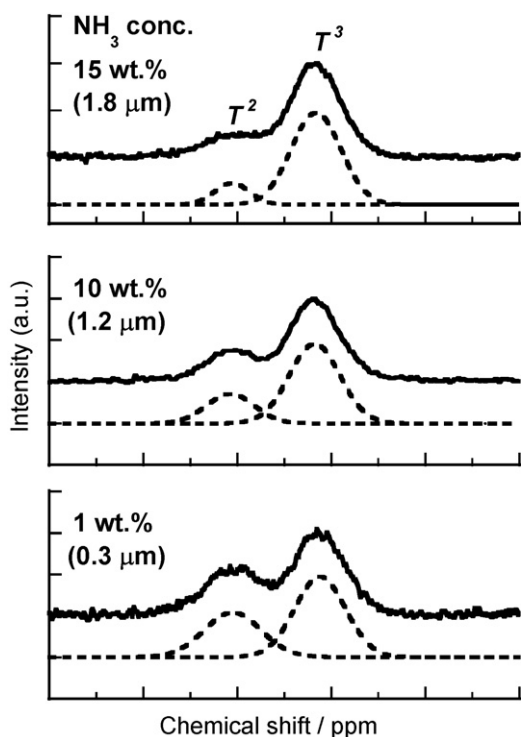
Fig. 3. Changes in ^{29}Si nuclear magnetic resonance spectra of PhSiO$_{3/2}$ particles with average particle diameter of 0.3, 1.2 or 1.8 μm.

3.3. Percolation of the PAMPS layer and proton conductivity

The volume fraction (ϕ) of multilayer in composite was calculated as follows:

$$V_{core} = \frac{4}{3}\pi r^3,$$
$$V_{core-shell} = \frac{4}{3}\pi R^3 = \frac{4}{3}\pi(r+d)^3,$$
$$\phi = \frac{V_{core-shell} - V_{core}}{V_{core-shell}} = 1 - \left(\frac{r}{R}\right)^3,$$

where V is the volume, r is the radius of PhSiO$_{3/2}$ particle, R is the radius of PAMPS-deposited particle, and d is the thickness of multilayer estimated from the QCM results (5 nm).

Shown in Fig. 7 is the relationship between the calculated ϕ and proton conductivity measured under 80% RH, and those values and the PhSiO$_{3/2}$ particle size were summarized in Table 2. The sam-
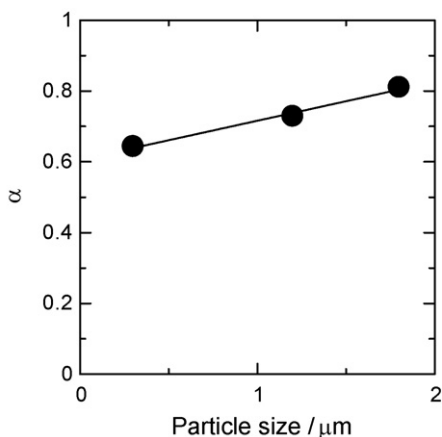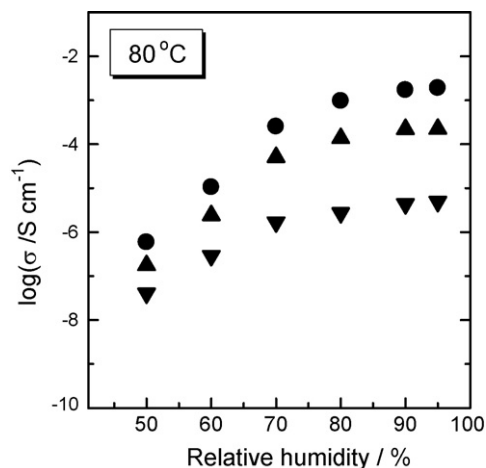

Fig. 5. Relative humidity dependences of proton conductivity for composite electrolytes prepared using PAMPS-deposited particles. The average core particle diameters are 0.25 μm (●), 0.5 μm (▲), and 1.8 μm (▼).
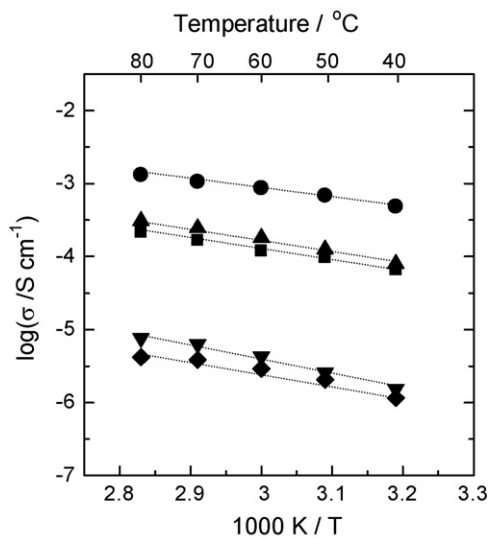

Fig. 6. Temperature dependences of proton conductivity at 80% RH for composite electrolytes prepared using PAMPS-deposited particles. The average core particle diameter are 0.25 μm (●), 0.5 μm (▲), 0.7 μm (■), 1.8 μm (▼) and 4.0 μm (♦).

Fig. 4. The relationship between the PhSiO$_{3/2}$ particle size and the calculated molar ratio (α) of T^3 unit.
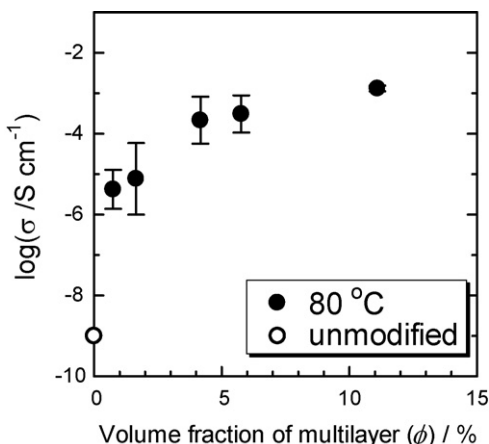

Fig. 7. Composition dependence of proton conductivity at 80% RH for composite electrolytes prepared using core size-controlled core–shell particles.

Table 2
The volume fraction of (PDDA/PSS/PDDA/PAMPS)-multilayer and proton conductivity at 80 °C and 80% RH for sheet-like samples.

Av. particle diameter (μm)	Volume fraction of multilayer (%)	Conductivity at 80 °C, 80% RH (S cm^{-1})
0.25	11.1	1.3×10^{-3}
0.5	5.7	3.1×10^{-4}
0.7	4.1	2.2×10^{-4}
1.8	1.6	7.7×10^{-6}
4.0	0.7	4.2×10^{-6}

ple prepared using unmodified $PhSiO_{3/2}$ particles exhibited a very low proton conductivity of 10^{-9} S cm^{-1} even at 80 °C. Note that the proton conductivity increased significantly for composites, and the composite with a multilayer volume fraction of ~1 vol.% exhibited approximately three orders of magnitude higher proton conductivity compared with the unmodified sample. The conductivity increased with increasing ϕ, and tended to gentle increase over around 5 vol.% of PAMPS-multilayer. The volume fraction of PAMPS-multilayer is directly related with the effective cross-sectional area of percolated proton conducting path in the composite electrolytes. The effective cross-sectional area of the conductive path increases with an increase in the volume fraction of PAMPS-multilayer, i.e., with a decrease in core particle size because the thickness of the multilayer is constant.

Theoretically, the percolation threshold of composites is around 16 vol.%, thus the ionic/electronic conductivity of composite samples increases drastically over $\phi = 0.16$ [22–24]. On the other hand, it is noteworthy that the proton conductivity of the composite electrolyte prepared in this study increased significantly with a very small amount of PAMPS (~1 vol.%). The advantage of composites prepared via LBL is that the proton conducting PAMPS layer is concentrated at the particle interfaces, which extended and percolated throughout the sheet-like samples. A considerable improvement in proton conductivity thus can be achieved with a relatively small amount of PAMPS, leading to a high proton conductivity and good chemical stability.

4. Conclusion

Proton conducting PAMPS ultrathin layer was deposited on sol–gel-derived $PhSiO_{3/2}$ particles via LbL assembly technique. The particle diameters of $PhSiO_{3/2}$ was controlled in the range of 0.25–4.0 μm by varying the concentration of NH$_4$OH catalyst. ^{29}Si NMR analysis revealed that the ratio of T^3 unit, which is monitored by the α value, was increased with an increase in the $PhSiO_{3/2}$ particle size. One PAMPS layer with 1.5 nm thickness was deposited on the particle via LbL assembly. A considerable improvement in proton conductivity can be achieved with a small amount of

PAMPS. This is ascribed to the PAMPS layer being concentrated at the particle interfaces, which percolated throughout the pelletized monolithic sample. Proton conductivity of the composite electrolyte reached 1.9×10^{-3} S cm^{-1} with 11.1 vol.% of multilayer at 80 °C and 95% RH. We anticipate that a multilayered ultrathin proton conductor is suitable as a fuel cell electrolyte with high proton conductivity and low fabrication cost.

References

[1] X. Lu, S. Wu, L. Wang, Z. Su, Sens. Actuators B 107 (2005) 812–817.
[2] W.J. Kim, D.-W. Kim, Electrochim. Acta 53 (2008) 4331–4335.
[3] K. Goto, I. Rozhanskii, Y. Yamakawa, T. Otuki, Y. Naito, Polym. J. 41 (2009) 95–104.
[4] M. Yamada, I. Honma, J. Phys. Chem. B 110 (2006) 20486–20490.
[5] M.L. Hill, Y.S. Kim, B.R. Einsla, J.E. McGrath, J. Membr. Sci. 283 (2006) 102–108.
[6] J.S. Lee, T. Nohira, R. Hagiwara, J. Power Sources 171 (2007) 535–539.
[7] P. Raghavan, X. Zhao, J.-K. Kim, J. Manuel, G.S. Chauhan, J.-H. Ahn, C. Nah, Electrochim. Acta 54 (2008) 228–234.
[8] S.H. Chung, Y. Wang, L. Persi, F. Croce, S.G. Greenbaum, B. Scrosati, E. Plichta, J. Power Sources 97–98 (2001) 644–648.
[9] F. Croce, L. Persi, B. Scrosati, F. Serraino-Fiory, E. Plichta, M.A. Hendrickson, Electrochim. Acta 46 (2001) 2457–2461.
[10] J. Adebahr, N. Ciccosillo, Y. Shekibi, D.R. MacFarlane, A.J. Hill, M. Forsyth, Solid State Ionics 177 (2006) 827–831.
[11] S. Furusawa, S. Shimizu, K. Sekine, H. Tabuchi, Solid State Ionics 167 (2004) 325–329.
[12] N. Sata, N.Y. Jin-Phillipp, K. Eberl, J. Maier, Solid State Ionics 154–155 (2002) 497–502.
[13] A. Peters, C. Korte, D. Hesse, N. Zakharov, J. Janek, Solid State Ionics 178 (2007) 67–76.
[14] S. Mühlherr, K. Läuger, E. Schreck, N. Zakherov, J. Janek, Solid State Ionics 28–30 (1988) 1495–1505.
[15] N. Kuwata, N. Sata, T. Tsurui, H. Yugami, Jpn. J. Appl. Phys. 44 (2005) 8613–8618.
[16] Y. Daiko, K. Katagiri, K. Shimoike, M. Sakai, A. Matsuda, Solid State Ionics 178 (2007) 621–625.
[17] Y. Daiko, H. Sakamoto, K. Katagiri, H. Muto, M. Sakai, A. Matsuda, J. Electrochem. Soc. 155 (2008) B479–B482.
[18] Y. Daiko, S. Sakakibara, H. Sakamoto, K. Katagiri, H. Muto, M. Sakai, A. Matsuda, J. Am. Ceram. Soc. 92 (2009) S185–S188.
[19] H. Sakamoto, Y. Daiko, K. Katagiri, H. Muto, M. Sakai, A. Matsuda, Solid State Ionics 181 (2010) 210–214.
[20] A. Matsuda, T. Sasaki, K. Hasegawa, M. Tatsumisago, T. Minami, J. Ceram. Soc. Jpn. 108 (2000) 830–835.
[21] J. Zhou, R.F. Childs, A.M. Mika, J. Membr. Sci. 254 (2005) 89–99.
[22] D.S. McLachlan, M. Blaszkiewicz, R.E. Newnham, J. Am. Ceram. Soc. 78 (1990) 2187–2203.
[23] F.C. Fonseca, R. Muccillo, Solid State Ionics 166 (2004) 157–165.
[24] K. Nozaki, T. Itami, J. Phys. Condens. Matter 18 (2006) 3617–3627.